Recent progress in metasurfaces: An introductory note from fundamentals and design methods to applications

Wei Chen[1, 2, #], Jiaqing Shen[1, 2, #], Yujie Ke[2], Yuwei Hu[2], Lin Wu[3,4,*], Jinfeng Zhu[1,*], Zhaogang Dong[2, 5,*]

[1]Institute of Electromagnetics and Acoustics and Key Laboratory of Electromagnetic Wave Science and Detection Technology, Xiamen University, Xiamen, Fujian, 361005 P. R. China

[2]Institute of Materials Research and Engineering (IMRE), Agency for Science, Technology and Research (A*STAR), 2 Fusionopolis Way, Innovis #08-03, Singapore, 138634 Republic of Singapore

[3]Science, Mathematics, and Technology (SMT), Singapore University of Technology and Design (SUTD), 8 Somapah Road, Singapore 487372

[4]Institute of High Performance Computing, A*STAR (Agency for Science, Technology, and Research), 1 Fusionopolis Way, No. 16-16 Connexis, Singapore 138632

[5]Department of Materials Science and Engineering, National University of Singapore, 9 Engineering Drive 1, 117575, Singapore

[#] These authors contributed equally

*Corresponding authors: Lin Wu, lin_wu@sutd.edu.sg; Jinfeng Zhu, jfzhu@xmu.edu.cn; Zhaogang Dong dongz@imre.a-star.edu.sg

Abstract

Metasurfaces refer to the sub-wavelength nanostructures that are capable of manipulating the amplitude, phase, polarization, and other characteristics of light, to enable diverse applications across the ultraviolet, visible, infrared, and terahertz spectra. In this review paper, we aim to provide an introductory note on metasurfaces, from fundamentals and design methods to applications, such as biosensing, environmental monitoring, metalenses, optical cloaking, electromagnetic scattering, structural color, miniaturized devices, and others. Moreover, we also identify the key challenges and limitations of metasurfaces, such as fabrication, integration, optimization, tuning, signal processing, and analysis, and suggest possible directions and solutions for future research. At last, we envision several emerging and promising trends for metasurfaces, such as new materials and structures, new phenomena and mechanisms, machine learning, and artificial intelligence techniques. The review is expected to inspire future development in this exciting and rapidly evolving field of metasurface devices.

Keywords: metamaterial, metasurface, deep learning, nanophotonics

1 Introduction

Natural materials exhibit limited capabilities to achieve arbitrary manipulation of electromagnetic waves [1-20]. As artificially aligned arrays at microscopic and nano scales, metamaterials offer a unique opportunity for tunable properties of electromagnetic, mechanics, acoustics, thermodynamics, and nanophotonics, as shown in Fig. 1(a) [21-45]. Through deliberate designs and precise arrangements of subwavelength elements, metamaterials can exhibit various exotic electromagnetic properties, such as negative refractive index, perfect light absorption, and nanoscale electromagnetic manipulation, which are rarely found in nature [46-70]. The typical configuration of metamaterials is volumetric, with their design and fabrication being highly complex, making miniaturization and integration challenging.

In 2011, Yu et al. proposed a two-dimensional array of optical resonators with spatially varying phase response and subwavelength separation, which could imprint such phase discontinuities on propagating light as it traverses the interface between two media [71]. After that, metasurfaces have emerged as a revolutionary technology, promising precise control over light at the subwavelength scale [72-81]. In general, metasurfaces are regarded as the two-dimensional counterpart of metamaterials, consisting of artificial structures on a flat surface in periodic or aperiodic arrangements [81-92]. This field has developed rapidly since 2011, giving rise to an increasing versatility and potential of metasurfaces in diverse applications, including the generation of orbital angular momentum, metalens architecture, optical cloaking, anomalous reflection, quantum information processing, and electromagnetic scattering [93-110]. Metasurfaces have experienced a fast development in design methodologies, underlying principles, and numerous applications spanning various disciplines. In addition, the continuous advancement of nanofabrication technology also contributes to discovering some novel physical properties of metasurfaces [111]. Significant progress has been made in realizing extreme light confinement and control in non-centrosymmetric phonon-polaritonic crystals [112]. Notable developments include out-of-plane hyperbolicity in uniaxial crystals, enabled by generating hyperbolic phonon polaritons in van der Waals materials. Additionally, surface anisotropy in cut crystals has generated ghost polaritons and leaky polaritons. Furthermore, investigating phonon polaritons in orthorhombic crystals with biaxial optical response has revealed valuable insights. The concept of twist-optics, exploiting the control of the propagation of phonon polaritons through twisted bilayer and trilayer van der Waals stacks, has also been thoroughly discussed [112-113]. In addition, some coupling modes (e.g., bound states in the continuum (BIC)) and multipole resonances (e.g., toroid dipole and anapole) are also explored [114-115]. These new physical properties significantly enhance the ability of light to interact with matter and expand the means of electromagnetic regulation. Therefore, it is very important to summarize recent progress in metasurface design.

Our goal is to provide readers with an introductive and comprehensive understanding of the latest advancements in metasurface research, covering fundamental theoretical frameworks, design methods, and practical implementations. Fig. 1(b) outlines the review content with a systematic examination of the fundamental design principles that underpin metasurface application and engineering. We introduce the two main design methods of forward and reverse designs, summarize their technical means, and discuss their advantages and disadvantages. The intricate interplay between design parameters (materials, structures, and design methods) and optical functionalities is examined. Then, we introduce various physical principles, including surface plasmonic resonance (SPR), cavity resonance, BIC, etc. By explaining the physical principles governing metasurface behavior, we aim to equip researchers and engineers with knowledge for the informed design towards specific applications, encompassing the fields ranging from communication, sensing, and imaging to energy harvesting. Whether applied to beam shaping, polarization manipulation, or designing ultrathin optical components, metasurfaces are providing disruptive technologies towards realizing compact and efficient photonic solutions. At last, we will share our opinions regarding the future directions for metasurface research.

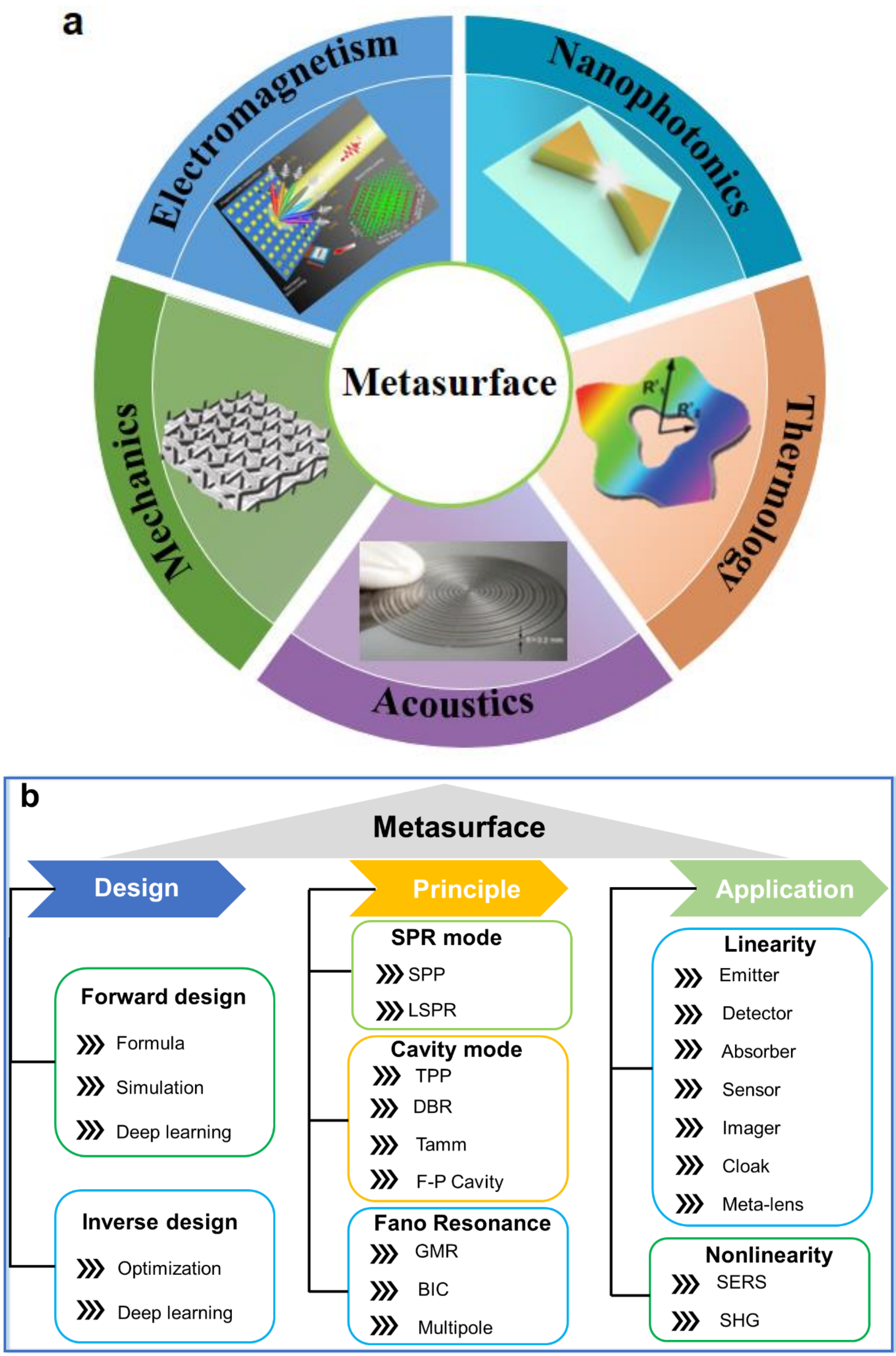

Fig. 1 Overview of metasurface research. (a) Applications of metasurfaces in various

disciplines, including mechanics, acoustics, thermodynamics, nanophotonics, electromagnetism, etc. [25-28] Copyright 2018, Nature. Applying for a license of figures. Copyright 2023, Wiley. Applying for a license of figures. Copyright 2021, Elsevier. Applying for a license of figures. Copyright 2022, Elsevier. Applying for a license of figures. (b) Overview of various design methods, principles, and applications for optical metasurfaces.

2 Resonance mechanisms

Resonances are the cornerstone of photonics [80], since the resonance mechanisms are critical for metasurfaces and related optical engineering applications, as shown in Fig. 2. One of the classic resonance mechanisms is the surface Plasmon Resonance (SPR) as supported on metal/dielectric nanostructures, including surface plasmon polariton (SPP) and localized surface plasmon resonance (LSPR) [116]. SPR is an electromagnetic phenomenon occurring at the interface between a metal and a dielectric, in which electromagnetic waves interact with oscillations of free electrons on metal surface. SPP is formed through the resonant oscillations between incident light and free electrons along a metal surface, when light is incident onto the metal surface at an appropriate angle. The frequency of this resonance is determined by the refractive index of the metal and the wavelength of the incident light. In addition, LSPR is a localized form of plasmon resonance occurring at the confined surface of metal nanostructures. When the sizes of metal nanoparticles are smaller than the wavelength of the incident light, LSPR can be supported around the sharp corners or tips around the nanostructures, inducing strongly enhanced localized electromagnetic fields. This phenomenon promotes the enhanced absorption and/or scattering in certain wavelengths [117], and therefore SPR has wide applications in biosensing, optical imaging, energy, and nanophotonics fields.

At the interface of the metal film and a one-dimensional photonic crystal, an electromagnetic surface state emerges, known as the Tamm plasmon polariton (TPP), like the electronic surface state envisaged by Tamm [118]. The dispersion characteristics of TPP enable direct excitation using both TE- and TM-polarized light from free space without the need for external momentum compensation. Due to its robust localization and slow light attributes, TPP offers significant potential for diverse applications, such as perfect absorbers, solar cells, narrow-band thermal emission, non-linear optical effects, and laser technologies [118].

The 3rd resonance that we introduced here is Fano Resonance, which is a quantum mechanical phenomenon being characterized by an asymmetric spectral line shape, originally proposed by Italian physicist Giovanni Fano in 1961 [119]. This resonance occurs when a discrete quantum state interferes with a continuum of states, resulting in a distinctive asymmetric profile in the resonance curve. Fano Resonance includes several key features, such as asymmetric line shape, interference phenomenon, and unique signatures of having a narrow peak with a broad background, where a compressive review on Fano resonance in optics is by Boris Luk'yanchuk, et al [120]. Besides optics, Fano Resonance is also encountered in other physical systems, including quantum mechanics, and condensed matter physics. Taking advantage of its peculiar spectral characteristics. It has practical applications in photonic fields, such as sensors and light filters. It's worth noting that the recently popular bound-states-in-the-continuum (BIC) resonance is also a type of Fano resonance, where the BIC resonance can be referred to more focused review and will not be repeated here.

The phonon polaritons are hybrid light–matter excitations of polar crystals and have arisen significant interest. Phonon polaritons exhibit extreme optical anisotropy and directionality, allowing new nanoscale light propagation and manipulation regimes. The role of crystal symmetry in determining the polariton response and associated phenomena are discussed, such as hyperbolic, ghost, and shear polaritons [121, 122]. The article further explores the emerging directions of polaritons in lower-symmetry materials and metamaterials, such as twist optics, topological physics, and nonlinearities [121, 123-126].

Multiple resonances describe different modes of electromagnetic oscillations in a system, being characterized by the distribution of electric and magnetic fields. Here, we present a brief introduction to some different modes of multipole resonances:

(1) Electric dipole resonance: This mode is associated with oscillating positive and negative charges in a linear or non-linear structure. In this mode, the electric field dominates, and the charges experience a shift, leading to an oscillation that resonates with the incident electromagnetic field.

(2) Magnetic dipole resonance: This mode involves oscillating magnetic moments under an external electromagnetic field. The magnetic field is dominant in this mode, and the system behaves like a magnetic dipole to experience resonance with the incident magnetic field.

(3) Toroid dipole resonance: This mode is characterized by an oscillation of currents circulating in a toroidal (doughnut-shaped) structure. Toroidal geometries can support resonances with unique properties and are used in applications such as metamaterials and electromagnetic devices.

(4) Anapole resonance: This mode is a unique type of resonance, in which the electric and magnetic fields are arranged to cancel each other out, leading to a total absence of outgoing radiation. The term "anapole" is derived from Greek, meaning without poles. Anapole resonances are of interest in the design of low-scattering or stealthy structures. These multipole resonances have distinct characteristics and applications [115, 127]. Understanding and controlling these resonances is crucial for tuning the optical and electromagnetic properties of metasurfaces.

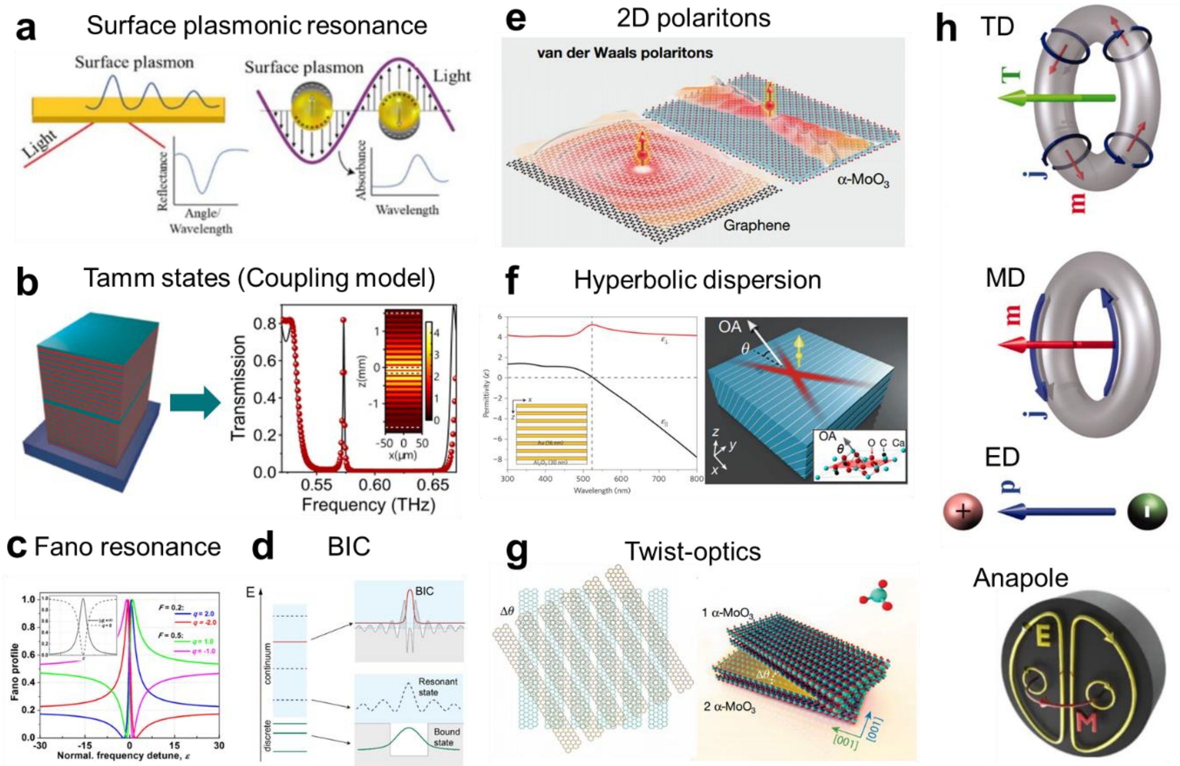

Fig. 2 Different physical mechanisms of metasurfaces. (a) Surface plasmonic resonance, including surface plasmonic polaritons (left) and local surface plasmonic resonance (right). [116] Copyright 2023, Beilstein-Institut. Applying for a license of figures. (b) Tamm states, a physical phenomenon associated with surface waves. [118] Copyright 2021, Elsevier. Applying for a license of figures. (c) Fano resonance usually occurs when a system has two different coupling modes [119]. Copyright 2018, Nature. Applying for a license of figures. (d) Bound

states in a continuum, a kind of resonant state. [120] Copyright 2016, Nature. Applying for a license of figures. (e) Van der Waals polaritons. [121] Copyright 2021, Nature. Applying for a license of figures. (f) Hyperbolic dispersion via artificial metamaterials (left) and natural materials (right). [112,122] Copyright 2023, Nature and 2016, Nature. Applying for a license of figures. (g) Twist-optics: controlling the propagation of phonon polaritons with twisted bilayer and trilayer stack. [121] Copyright 2021, Nature. Applying for a license of figures. (h) Different modes of multipole resonance, including toroid dipole, magnetic dipole, electric dipole, and anapole. [115, 127] Copyright 2010, AAAS and 2015, Nature. Applying for a license of figures.

3 Design methods

In this section, we are providing a comprehensive overview of the design methods as facilitated by computing machinery, as shown in Fig. 3. The design methodologies are mainly classified into forward and inverse design, e.g., from structural parameters to optical response and prediction of structural parameters based on demand. The development of nanophotonics has achieved remarkable results in both categories.

Regarding forward design, analytic formulas are based on mathematical formulas, such as the transfer matrix method (TMM) and Mie scattering theory [128,129]. TMM analyzes the light propagation of layered structures using the transfer matrix method, and Mie's theory focuses on the scattering and absorption of spherical particles. Moreover, simulation methods also rely on computer simulation, such as finite-difference time-domain (FDTD), rigorous coupled-wave analysis (RCWA), and finite element method (FEM), which use simulation tools to analyze the optical properties of nanostructures, providing researchers with flexible and intuitive means [130,131].

On the other hand, inverse design methods aim at predicting structural parameters according to desired optical properties. In terms of optimization algorithms, particle swarm optimization, genetic algorithms, and simulated annealing are widely used [132]. These algorithms search for the optimal solution in different ways, *e.g.*, simulating the processes of bird flocks (biological evolution) and metal annealing in nature to provide an efficient way to design nanophotonics. The advancement in metasurface inverse design has led to enduring scientific innovations. Deep learning (DL) technologies, such as artificial neural networks and generative pre-trained transformers (GPT), are flourishing in scientific discovery and intelligent design. Researchers have also utilized a variety of sophisticated neural network architectures to propel metamaterial design forward, including multilayer perceptrons, convolutional neural networks, recurrent neural networks, generative adversarial networks, and transformer networks. Deep learning, as an emerging design methodology, incorporates neural network structures like multilayer perceptrons, transformers, convolutional neural networks, etc., facilitating smarter and faster nanostructure design processes [133]. Next, we will discuss the advances of deep learning in metasurface design.

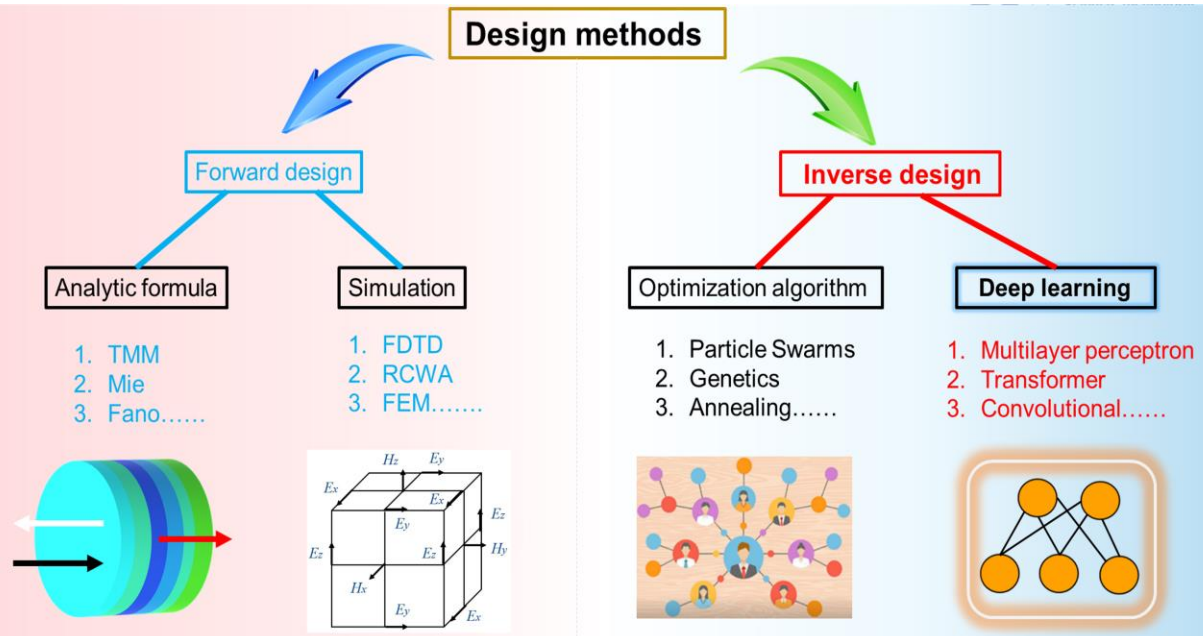

Fig. 3 Forward and inverse design methods for metasurface devices, including analytic formula, simulation tool, optimization algorithm, and deep learning.

Deep learning (DL) is crucial in metasurface design, customization, and optimization in photonics. For instance, DL is a subset of machine learning that can learn multilevel abstraction of data with hierarchically structured layers. It complements conventional physics- and rule-based methods. Zhu et al. presented a DL scheme based on a divide-and-conquer strategy for the on-demand design of circuit-analog plasmonic stack metamaterials, as shown in Fig. 4a [30]. This method splits a spectrum into several parts and demonstrates higher precision for the spectral prediction of the plasmonic stack metamaterial (PSM) structure. The DL method uses fewer training parameters than the conventional method of the fully connected network. Using this approach, the entire bidirectional network achieves precise inverse design.

In addition, Soljačić et al. developed a method using artificial neural networks (N.N.) to approximate light scattering by multilayer nanoparticles, as shown in Fig. 4b [134]. Only a small sampling of training data is required for the network to achieve high precision in approximating the simulation. Once trained, the neural network can simulate optical processes much faster than conventional methods. For instance, Chen et al. proposed a DL method based on a metamaterial spectrum transformer (MST) for the powerful design of high-performance solar metamaterial absorbers (SMAs), as shown in Fig. 4c [1]. The MST divides the optical spectrum of metamaterial into several patches, solving the problem of overfitting in traditional DL and significantly boosting learning capability. A flexible design tool that allows user-defined specifications is developed to enable real-time and on-demand design of metamaterials with various optical functions. This scheme is applied to designing and fabricating SMAs with graded-refractive-index nanostructures, exhibiting a high average absorptance of 94% in a broad solar spectrum and significant advantages over many state-of-the-art counterparts.

Qian et al. proposed the concept of an intelligent cloak driven by DL and introduced a metasurface cloak as an example implementation, as shown in Fig. 4d [135]. The metasurface cloak exhibits a millisecond response time to changing incident waves and the surrounding environment in experiments. This work brings to a wide range of real-time and in-situ applications, such as moving stealth vehicles. Chen et al. proposed a Q-BIC based all-dielectric metasurface using a transformer-based DL network for SERS spectroscopic applications, as shown in Fig. 4e [2]. By manipulating the incident angle, a mechanism based on strong coupling Q-BIC is achieved with a large Rabi splitting of ≈105 meV, which creates a bandgap and forms an anti-crossing behavior. Compared to conventional methods, the strong coupling Q-BIC scheme provides an extraordinary SERS enhancement factor of $\sim 10^{17}$ and extends the field-enhancing scale up to ten times. Ma et al. applied statistical machine learning in designing and optimizing complex multifunctional metasurfaces, as shown in Fig. 4f [136]. In contrast to the traditional two-step approach, which separates phase retrieval and meta-atom structural design, the proposed end-to-end framework effectively utilizes the prescribed design space and pushes the multifunctional design capacity to its physical limit. With a single-layer structure, metasurface focusing lenses and holograms are experimentally demonstrated in the near-infrared region. It exhibits up to eight controllable responses for different combinations of working frequencies and linear polarization states, which are impossible by using conventional physics-guided approaches [136].

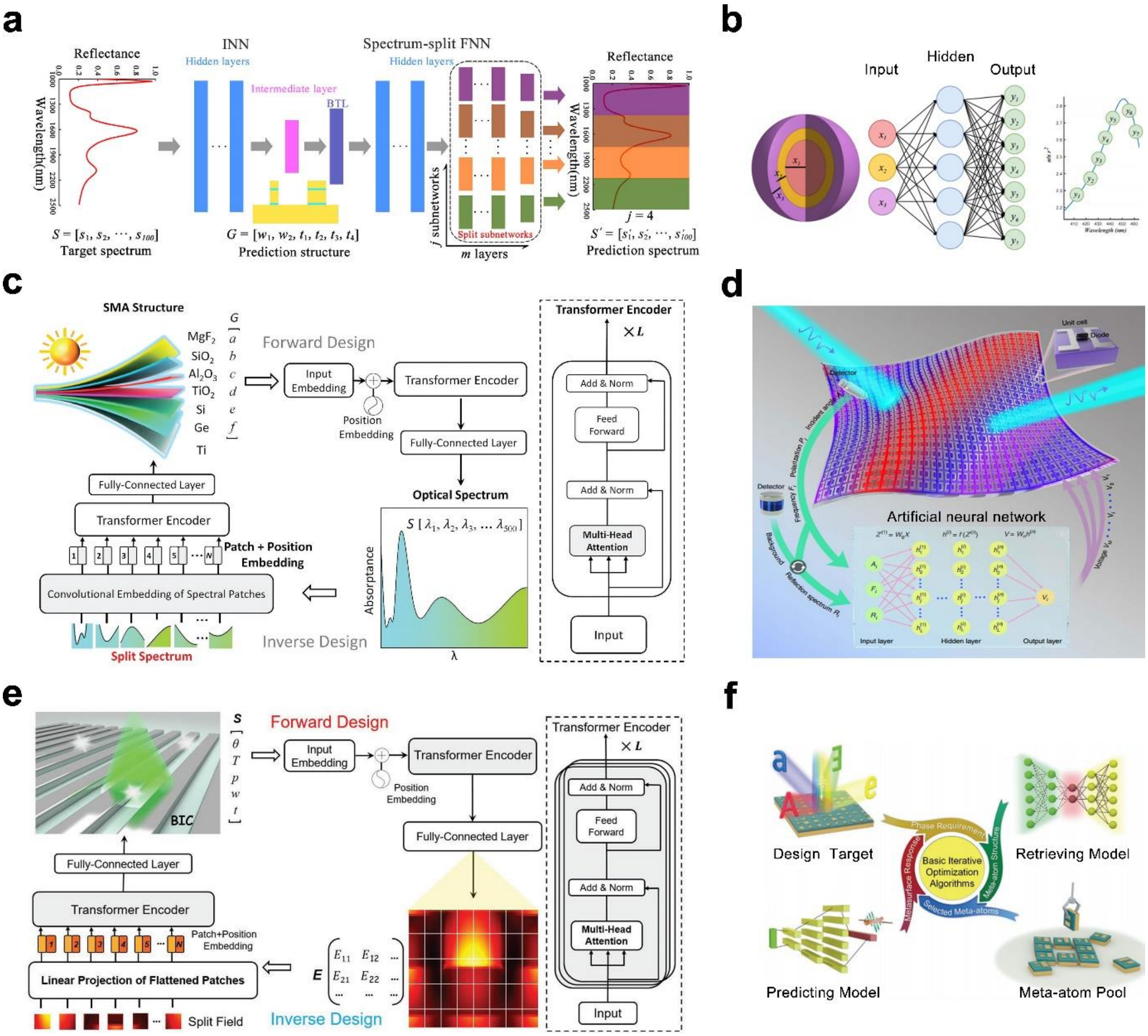

Fig. 4 Deep learning empowering and accelerating the metasurface design. (a) The architecture of divide-and-conquer DL based on a bidirectional artificial neural network [30]. Copyright 2023, Wiley. Applying for a license of figures. (b) The N.N. architecture has as its input the thickness of each nanoparticle shell and, as its output, the scattering cross-section at different wavelengths of the scattering spectrum [134]. Copyright 2018, AAAS. Applying for a license of figures. (c) MST architecture for the smart design of graded-refractive-index-based SMAs. Adapted with permission. [1] Copyright 2023, Wiley. 2. Applying for a license of figures. (d) A deep-learning-enabled self-adaptive metasurface cloak. Adapted with permission.

[135] Copyright 2020, Nature. Applying for a license of figures. (e) The architecture of the transformer-based model. Adapted with permission. [2] Copyright 2023, Wiley. Applying for a license of figures. (f) End-to-end design pipeline for multifunctional metasurfaces. Adapted with permission. [136] Copyright 2022, Wiley. Applying for a license of figures.

4 Advanced applications based on metasurfaces

In this section, diverse applications of metasurfaces are discussed, showcasing the multifaceted utility and burgeoning research in this field (Fig. 5). These applications include linear and non-linear optical engineering, such as perovskite emission engineering and controlling, second harmonic generation, surface-enhanced Raman spectroscopy, miniaturized lasers, and so on [137-148]. For instance, Csányi et al. reported on a method to engineer and shift the photoluminescence wavelength of $FAPbI_3$ perovskite quantum dots (QDs) by using optical nanoantenna arrays driven by quasi-BIC resonances via Purcell effect [139]. This method provides a non-invasive and non-destructive way to tune the emission properties of perovskite QDs.

Ho et al. presented a design of color-sensitive photodetectors based on hybrid silicon-aluminum nanostructures to achieve submicrometer pixel dimensions and minimize optical cross-talk [140]. These nanostructures have dual functionalities: (1) they exhibit a hybrid Mie-plasmon resonance to achieve color-selective light absorption and generate electron-hole pairs; and (2) create a Schottky barrier for photodetection and charge separation. The authors fabricated and characterized the color-sensitive photodetectors with varying nanodisk diameters and proved the photodetectors with a wavelength-dependent photoresponse and a high responsivity. The proposed design is promising to replace the traditional dye-based filters for camera sensors with ultrahigh pixel densities and extend the detection range to the ultraviolet (UV) regime.

Zhang et al. demonstrated chiral emission from resonant metasurfaces [147], where the authors designed and fabricated a resonant metasurface consisting of a square lattice of tilted titanium dioxide bars on an indium tin oxide–coated substrate. By introducing two asymmetry parameters, they could manipulate the positions and properties of C-points, where the circular polarization conversion occurs. The authors experimentally demonstrated chiral emission and lasing from the metasurface under different excitation conditions, achieving high-quality chiral emission with a near-unity degree of circular polarization, narrow divergence angle, and large circular dichroism. They further achieved chiral lasing with single-mode operation, high Q factor, and improved directionality. The authors proposed that their resonant metasurface can serve as an efficient and controllable source for chiral light generation for nanophotonics and quantum optics. Numerous applications based on metasurfaces have reached an advanced level of maturity, offering a wide range of advanced functionalities. However, due to space constraints in this introductory review, providing a comprehensive overview of each application is challenging. Nevertheless, our teams have gained extensive experience and unique insights in specific domains, such as structural colors, biosensing, and molecular fingerprint sensing over the years. Therefore, we will proceed to present the detailed and comprehensive introductions to these representative applications.

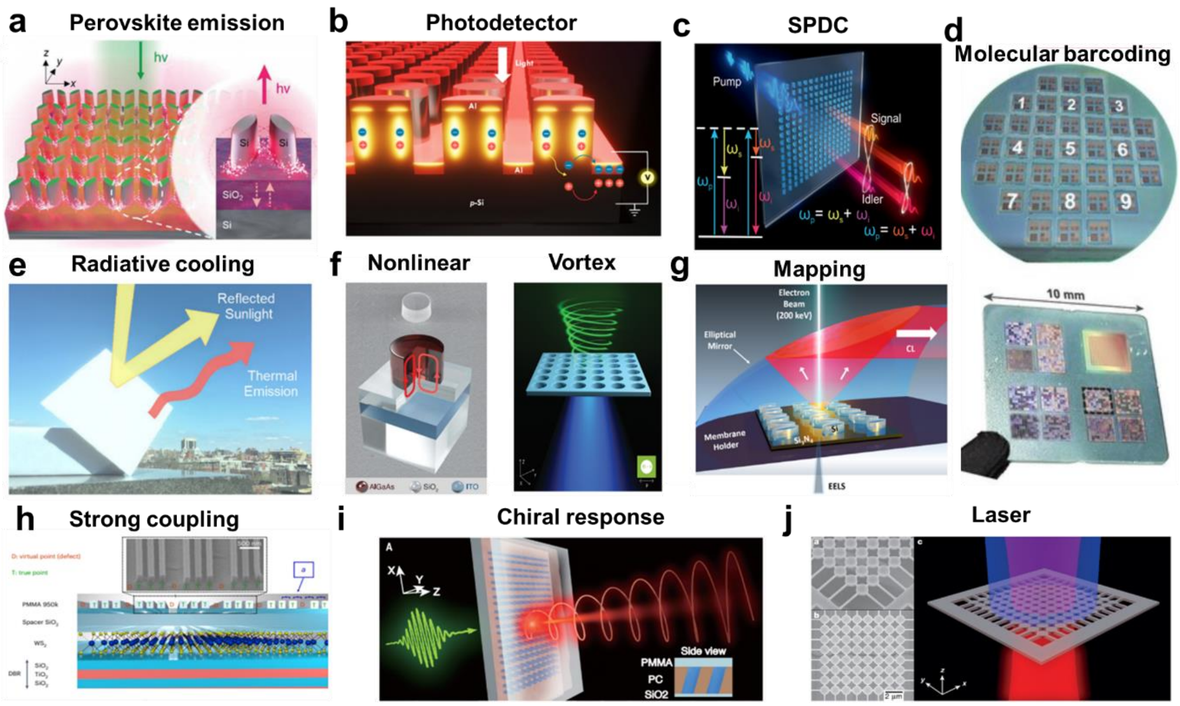

Fig. 5 Various applications enabled by metasurfaces. (a) Q-BIC antenna for engineering the perovskite QD emission characteristics. Adapted with permission. [139] Copyright 2024, Wiley. Applying for a license of figures. (b) Miniaturizing color-sensitive photodetectors via hybrid nanoantennas toward submicrometer dimensions. Adapted with permission. [140] Copyright 2022, AAAS. Applying for a license of figures. (c) Resonant metasurfaces for generating complex quantum states. Adapted with permission. [141] Copyright 2022, AAAS. Applying for a license of figures. (d) Imaging-based molecular barcoding with pixelated dielectric

metasurfaces. Adapted with permission. [142] Copyright 2021, Wiley. Applying for a license of figures. (e) Radiative cooling engineering. Adapted with permission. [139] Copyright 2018, AAAS. Applying for a license of figures. (f) subwavelength dielectric resonators for nonlinear nanophotonics and ultrafast control of vortex microlasers. Adapted with permission. [144-145] Copyright 2020, AAAS and 2020, AAAS. Applying for a license of figures. (g) Nanoscale mapping of optically inaccessible bound-states-in-the-continuum. Adapted with permission. [62] Copyright 2022, Nature. Applying for a license of figures. (h) Strong-enhanced light-matter coupling. Adapted with permission. [146] Copyright 2023, Nature. Applying for a license of figures. (i) Intrinsic chiral BIC. Adapted with permission. [147] Copyright 2022, AAAS. Applying for a license of figures. (j) Lasing action from photonic BIC. Adapted with permission. [148] Copyright 2017, Nature. Applying for a license of figures.

4.1 Structure Color

Structural color based on metasurface is an intriguing field that explores color generation through engineered structures rather than pigments, as shown in Fig. 6 [149-156]. This phenomenon originates from the intricate interactions between light and nanostructured surfaces. The metasurface design for structural color involves the unique geometric configurations and periodicities of nanostructures. By tailoring the geometrical parameters, one can precisely control the wavelengths of reflected or transmitted light to create highly saturated and customizable color palettes. Therefore, a myriad of vibrant colors can be expertly crafted and brought to life through precise manipulation of nanostructures, such as sizes, shapes, arrangements, and material compositions. Color generation by nanostructures has many advantages, such as energy-efficient non-emissive displays, high-resolution color printing, and novel optical sensors. In addition, the nanostructural color pixels can be tuned actively. For example, Lu et al. presented a reversible tuning approach for Mie resonances in the visible spectrum [152]. Moreover, metasurface with structural color can be used for anti-counterfeiting, due to its complex and distinctive patterns. For instance, the authors designed a tri-functional metasurface that can manipulate the phase, amplitude, and luminescence of light by using anisotropic gap-plasmon structures with upconversion nanoparticles (UCNPs) in their dielectric gap [156]. This metasurface can generate a color image under white light, a hologram under a red laser, and a luminescence image under a near-infrared (NIR) source, depending on the polarization of the incident light. It also exhibits a physically unclonable function (PUF) feature because of the stochastic distribution of the UCNPs, which creates a unique luminescence pattern for each metasurface. Therefore, it offers a highly secure and easy-to-authenticate optical anti-counterfeiting device, which combines the overt, covert, and forensic security features in a single planar device.

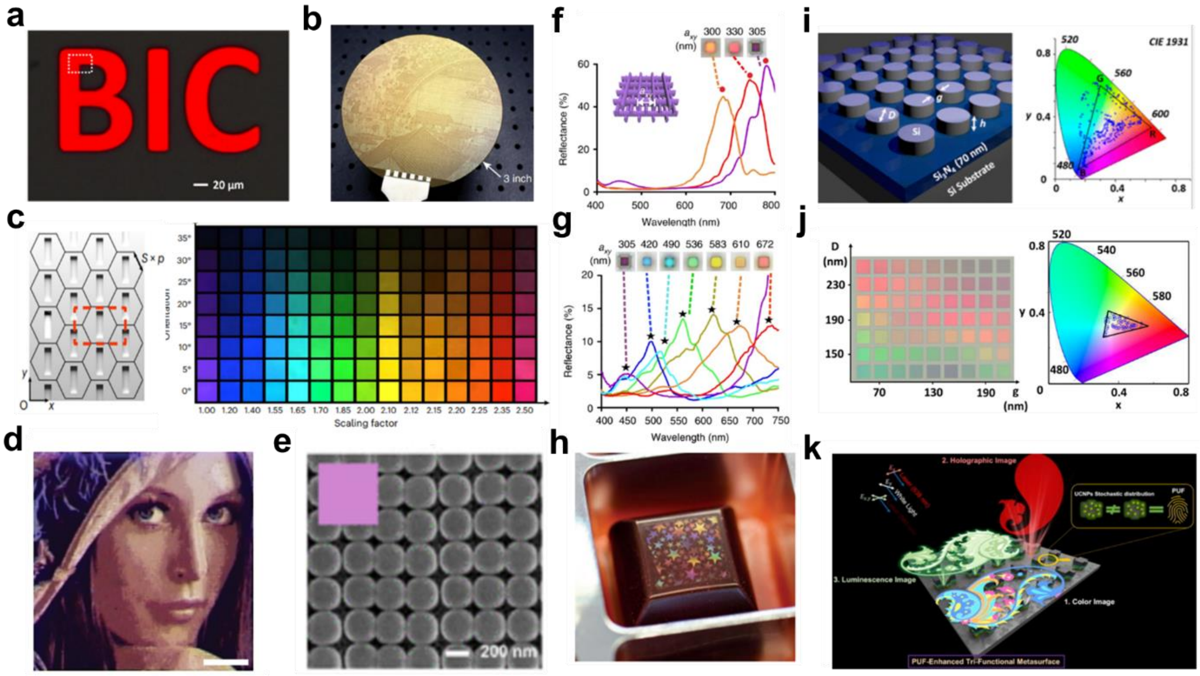

Fig. 6 Plasmonic and all-dielectric metasurfaces for structural color applications. (a) Schrödinger's red pixel by quasi-bound-states-in-the-continuum (q-BIC). Adapted with permission.[61] Copyright 2022, AAAS. Applying for a license of figures. (b) Spatial modulation of nanopattern dimensions by combining interference lithography and grayscale-patterned secondary exposure. Adapted with permission.[149] Copyright 2022, Nature. Applying for a license of figures. (c) Versatile full-color nanopainting enabled by a pixelated plasmonic metasurface. Adapted with permission. [150] Copyright 2023, Nature. Applying for a license of figures. (d) Printing color at the optical diffraction limit. Adapted with permission. [147] Copyright 2012, Nature. Applying for a license of figures. (e) Reversible Tuning of Mie Resonances in the Visible Spectrum. Adapted with permission. [152] Copyright 2021, ACS. Applying for a license of figures. Reflectance spectra and reflection-mode micrographs of woodpiles under top-down illumination conditions for (f) $a_{xy} = 300–350$ nm and (g) $a_{xy} = 350$-

672 nm, respectively. Structural color three-dimensional printing by shrinking photonic crystals. Adapted with permission. [153] Copyright 2019, Nature. Applying for a license of figures. (h) All colors originate solely from the surface nanotexture, which was replicated from corresponding structures on the surface of the chocolate mould. Adapted with permission. [154] Copyright 2017, Nature. Applying for a license of figures. (i) Printing beyond the sRGB color gamut by mimicking silicon nanostructures in free space. Adapted with permission. [60] Copyright 2017, ACS. Applying for a license of figures. (j) Reversible electrical switching of nanostructural color pixels. Adapted with permission. [155] Copyright 2023, De Gruyter. Applying for a license of figures. (k) Tri-functional metasurface enhanced with a physically unclonable function. Adapted with permission. [156] Copyright 2023, Elsevier. Applying for a license of figures.

4.2 Metasurface for biosensing applications

Metasurfaces have a strong near-field enhancement effect and are highly sensitive to changes in the refractive indices of surrounding environments. This characteristic is demonstrated by the resonance wavelength shift that occurs, when light interacts with the structures. These spectral changes can reflect microscopic information of the substances. Metasurface sensors have garnered significant attention in the academic community due to their excellent high sensitivity and fast, real-time, and label-free detection [157-159]. One can optimize the structural parameters of specific metasurface arrays and alter the incident light excitation conditions to improve the sensing performance of equipartition excitations. For instance, metasurfaces have been applied in various biosensing fields, including immunoassays [160-163], DNA-protein interactions [164], and real-time monitoring of antigen-antibody bindings [165-167].

Fig. 7a illustrates the label-free genetic screening technology proposed by Dionne et al. [168], which uses high-quality factor silicon nanoantennas functionalized with nucleic acid fragments. Each antenna has a resonant quality factor of ~2,200 in a physiological buffer. Altug et al. [169] developed a single-wavelength imaging biosensor, as shown in Fig. 7b, where it can reconstruct spectral shift information using an optimal linear estimator. These chips are coupled with microfluidics and arranged as microarrays on an imaging platform to detect real-time extracellular vesicles (EVs) associated with breast cancer. They have demonstrated a figure-of-merit of ~ 70 RIU^{-1}, and the system exhibits remarkable sensing capability of extracellular vesicle binding down to 0.41 nanoparticles/μm^2. Fig. 7c shows an analytical platform that uses circulating EVs to evaluate the activity of tumor-specific drug-target interactions in patient blood samples, where they monitor EV protein expression and small-molecule chemical occupancy and track various targeted therapies. They are able to identify EV signals that correspond closely to the effectiveness of cellular treatment. Moreover, metasurfaces also have the potential applications for clinical cancer prognosis and diagnosis. Zhu et al. [171] presented a highly effective affinity testing approach, as shown in Fig. 7d. They use label-free plasmonic metasurface sensors and monoclonal antibodies to test their binding affinity to 12 spike receptor binding domain (RBD) variants of SARS-CoV-2. In addition, they thoroughly analyze the molecular kinetics of the Langmuir binding equilibrium between the 12 SARS-CoV-2 RBD variants and mAb-functionalized metasurfaces.

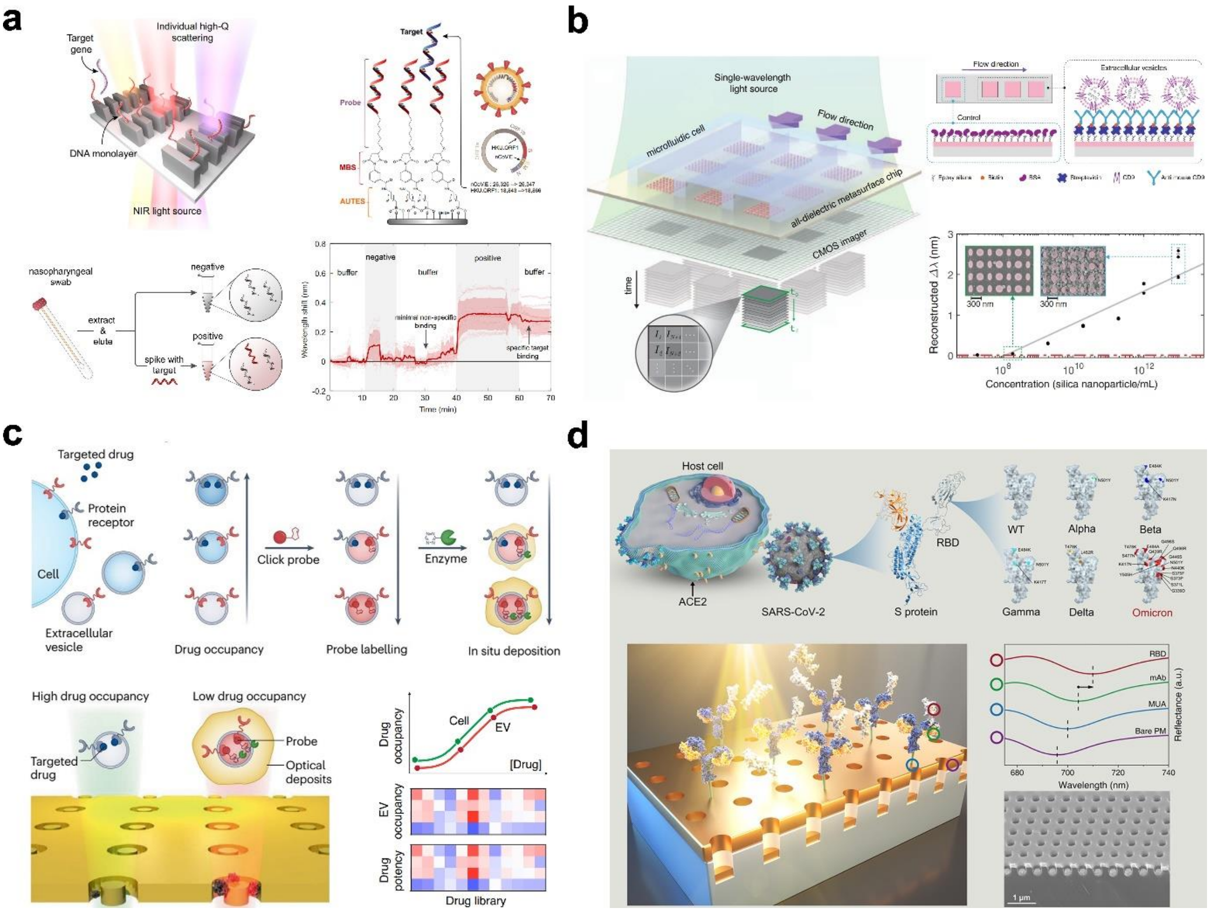

Fig. 7 Metasurface for biosensing applications. (a) Biosensing demonstration with SARS-CoV-2 gene fragment targets using metasurface arrays consisting of perturbed chains of silicon

blocks interfaced with DNA probes for targeted gene detection in clinical nasopharyngeal eluates. Adapted with permission. [168] Copyright 2023, Nature. Applying for a license of figures. (b) Biosensing using reconstructed spectral shift based on an aided imaging method. The new optofluidic device is applied for real-time detection of breast cancer-derived EVs by functionalizing the metasurfaces with specific antibodies. Adapted with permission. [169] Copyright 2021, Nature. Applying for a license of figures. (c) Assessment of EV-drug target interactions through bio-orthogonal probe amplification and spatial patterning of molecular reactions within EV size-matched plasmonic nanoring resonators, enabling in situ analysis of EV-drug dynamics. Adapted with permission. [170] Copyright 2021, Nature. Applying for a license of figures. (d) Detection of SARS-CoV-2 RBD variants using PMs with high-affinity monoclonal antibodies (mAbs). The PMs with multiple plasmonic modes are functionalized with diverse mAbs, and their molecular affinity characteristics to various SARS-CoV-2 RBD variants are systematically investigated. Adapted with permission. [171] Copyright 2023, ACS. Applying for a license of figures.

4.3 Metasurface for molecular fingerprint sensing applications

Because of molecular rotations and vibrations, many complex molecules exhibit characteristic absorption in the mid-infrared to terahertz spectrum. Surface-enhanced infrared absorption has gained significant attention in recent years, due to its advantages of low-loss, and high-Q factor resonances, which can enhance samples' absorption fingerprint spectral signatures for analyte identification [172-175]. Fig. 8a shows an imaging-based nanophotonic technique for identifying mid-infrared molecular fingerprints and its application for the chemical identification of surface-bound analytes. Altug et al. [176] presented a metasurface device for measuring the molecular absorption signatures at various spectral points, using a two-dimensional pixelated dielectric metasurface with various ultrasharp resonances, which can be tuned to a discrete frequency. The metasurface device can convert the spectral data into an imaging-ready spatial absorption map resembling a barcode. Fig. 8b shows a design for plasmonic nanofin metasurfaces that support symmetry-protected BIC up to the fourth order, developed by Maier et al. [177]. They obtain high-Q factor modes breaking the out-of-plane symmetry of the nanofins in parameter space. This symmetry breaking can be fine-tuned by adjusting the nanofins' triangle angle, providing a way to control the ratio of radiative to intrinsic losses precisely. Zhu et al. [13] presented an inverted dielectric metagrating for enhancing the broadband THz fingerprint detection of trace analytes on a planar sensing surface, shown in Fig. 8c. They tune the asymmetry parameter of quasi-BIC modes, so as to boost the near-field intensity within the analytes. The multiplexing mechanism for broadband detection is demonstrated by manipulating incident angles of excitation waves and the waveguide thickness. As a result, the THz fingerprint peak values are significantly enhanced compared to conventional approaches with a factor of up to 330-fold. Lyu and Chen [178] designed a frequency-selective fingerprint sensor (FSFS), as shown in Fig. 8d. This platform achieves enhanced trace fingerprint detection through broadband multiplexing. Its central wavelength is linearly related to the cross-slot length, and the broadband absorption lines of trace-amount chiral carnitine were boosted by 7.3 times.

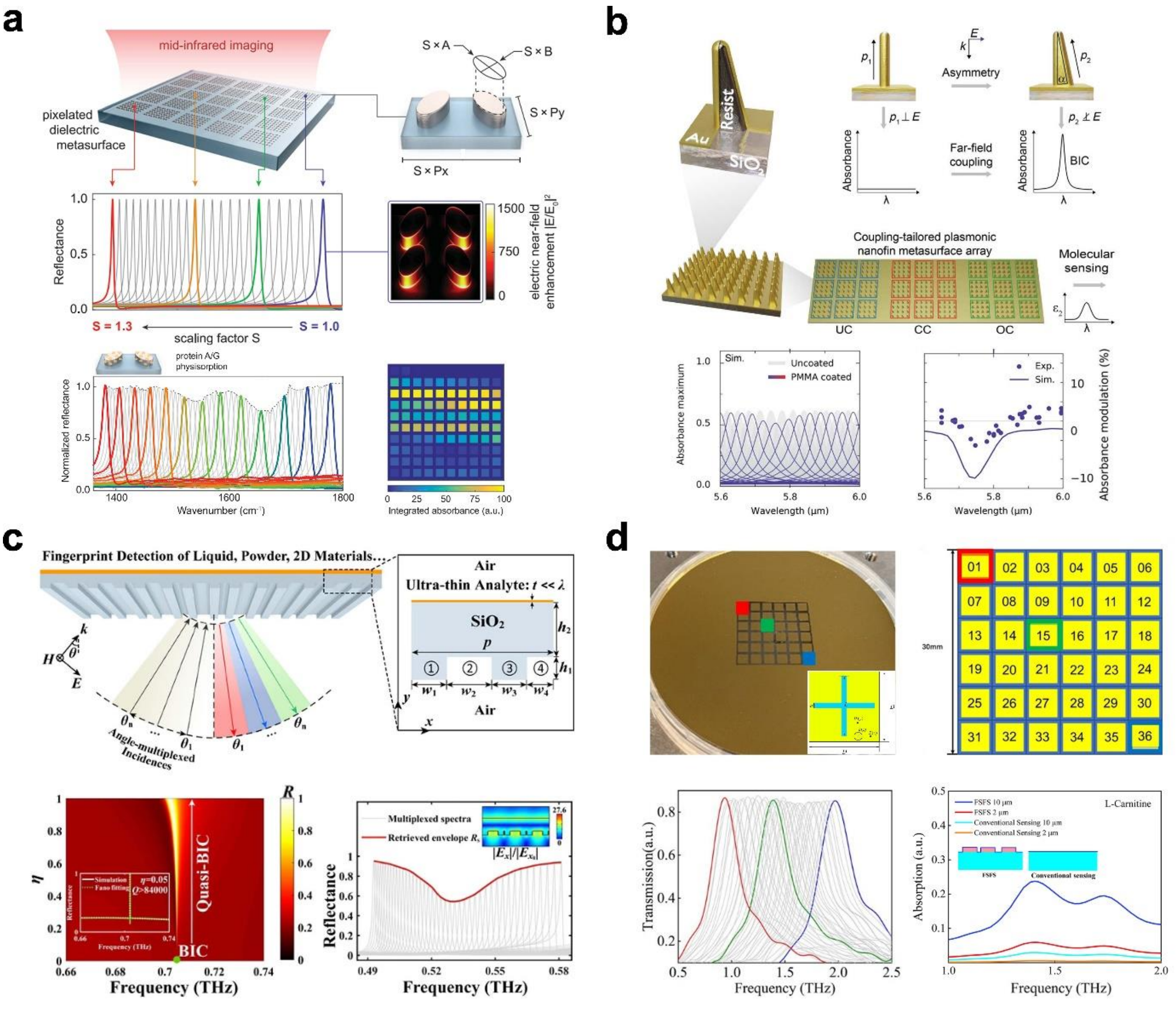

Fig. 8 Metasurface for molecular fingerprint sensing applications. (a) Molecular

fingerprint detection with pixelated dielectric metasurfaces. The pixelated metasurface is composed of a two-dimensional array of high-Q resonant megapixels with resonance frequencies tuned over a target molecular fingerprint range. Adapted with permission. [176] Copyright 2018, AAAS. Applying for a license of figures. (b) Plasmonic nanofin metasurfaces with coupling-tailored sensing. The absorbance spectra of uncoated (grey) and 5-nm PMMA-coated (colored) metasurfaces. Adapted with permission. [177] Copyright 2022, AAAS. Applying for a license of figures. (c) Enhancing THz fingerprint detection. The sensing enhancement is attributed to the use of evanescent waves at the planar air-metastructure interface for a series of quasi-BIC resonance modes. The broadband fingerprint signals of trace analytes can be retrieved by tuning the reflectance peaks. Adapted with permission. [13] Copyright 20222, OSA. Applying for a license of figures. (d) Enhanced absorption induced transparency by frequency selective fingerprint sensor. Optical images of the fabricated FSFS, with 36-pixel locations (P1-P36 corresponds to L from 104 μm to 47 μm), and measured transmission spectra of 10 μm thick L-carnitine coating on the FSFS, as well as the enveloped absorbance signals of L-carnitine. Adapted with permission. [178] Copyright 2023, Springer. Applying for a license of figures.

5. Insight and outlook

Metasurfaces are emerging as a powerful and versatile tool for various applications in the UV, visible, infrared, to terahertz spectral range [179-182]. By exploiting the strong near-field enhancements and high-Q factor resonances, these devices can achieve multiplexing and powerful capabilities, enabling a wide range of applications in biosensing, environmental monitoring, metalenses, optical cloaking, electromagnetic scattering, structural colors, miniaturized functional devices and others. However, at the same time, metasurface devices also face several challenges and limitations that must be addressed and overcome. These challenges include: (i) The fabrication and integration of metasurfaces with microfluidics, electronics, and optics, which require high precision, scalability, and compatibility. (ii) The optimization and tuning of metasurface parameters and excitation conditions require advanced designs and simulation methods and tools. (iii) The signal processing and analysis of metasurface spectra require efficient and robust algorithms and models.

To tackle these challenges and advance the field of metasurface sensors, we envision several possible directions and solutions for future research. These directions include: (i) Developing new materials and structures for metasurfaces, such as 2D materials, phase-change materials, and reconfigurable metasurfaces, which can offer new functionalities and properties for metasurfaces. (ii) Exploring new phenomena and mechanisms for metasurfaces, such as non-linear, quantum, and topological effects, can enhance performance. (iii) Applying machine learning and artificial intelligence techniques for metasurface design, such as deep learning, generative adversarial networks, and reinforcement learning, can improve the accuracy and efficiency of modeling. Furthermore, the frontier applications of intelligent algorithms and metasurfaces can be extended by introducing the concept of intelligent metamaterials. This involves utilizing metasurfaces to enable all-optical computing and integrating algorithms like artificial neural networks [183-185]. Metasurface devices are at the forefront of nanotechnology and optics, offering innovative solutions for advanced applications. We believe that metasurface devices have great potential and promise for advancing science and technology and benefiting society and humanity. We hope this review can provide a useful and introductory reference for researchers and practitioners interested in and working on metasurfaces and inspire them to explore new possibilities and opportunities in this exciting and rapidly evolving field.

Conflict of Interest

The authors declare no conflict of interest.

Acknowledgments

Z.D. would like to acknowledge the funding support from the Agency for Science, Technology and Research (A*STAR) under its AME IRG (Project No. A20E5c0093), Career Development Award grant (Project No. C210112019), MTC IRG (Project No. M21K2c0116 and M22K2c0088), the Quantum Engineering Programme 2.0 (Award No. NRF2021-QEP2-03-P09) and DELTA-Q 2.0 (Project No. C230917005). J.Z. would like to acknowledge the funding support from NSFC (62175205), NSAF (U2130112) and the Youth Talent Support Program of Fujian Province (Eyas Plan of Fujian Province) [2022]. W. C. would like to acknowledge the funding supporting from the China Scholarship Council Scholarship (CSC NO. 202306310153). J. S. would like to acknowledge the funding supporting from the China Scholarship Council Scholarship (CSC NO. 202306310168).

Reference

1. W. Chen, Y. Gao, Y. Y. Li, et al., *Advanced Science,* 2023, **10**, 2206718.
2. W. Chen, Y. Y. Li, Y. E. Liu, et al., *Advanced Optical Materials,* 2023, **12,** 2301697.
3. S. Ding, J. Y. Ou, L. H. Du, et al., *Carbon,* 2021, **179**, 666-676.
4. M. Gao, W. M. Yang, Z. Y. Wang, et al., *Photonics Research,* 2020, **8**, 1226-1235.
5. S. C. Huang, X. Wang, Q. Q. Zhao, et al., *Nature Communications,* 2020, **11**, 4211.
6. T. X. Huang, C. W. Li, L. K.Yang, et al., *Nanoscale,* 2018, **10**, 4398-4405.
7. F. F. Jiao, F. J. Li, J. Q. Shen, et al., *Sensors and Actuators B-Chemical,* 2021, **344**, 130170.
8. C. W. Li, J. L. Qiu, J. Y. Ou, et al., *ACS Applied Nano Materials,* 2019, **2**, 3231-3237.
9. F. J. Li, J. Q. Shen, C. H. Guan, et al., *Biosensors & Bioelectronics,* 2022, **203**, 114038.
10. B. W. Liu, S. Chen, J. C. Zhang, et al., *Advanced Materials,* 2018, **30**, 1706031.
11 H. Liu, C. Koyama, J. Zhu, et al., *Remote Sensing,* 2016, **8**, 935.
12. J. L. Liu, X. Li, R. R. Jiang, et al., *Sensors,* 2021, **21**, 4987.
13. X. Y. Liu, W. Chen, Y. J. Ma, et al., *Photonics Research,* 2022**, 10**, 2836-2845.
14. X. R. Mao, Y. F. Hang, Y. G. Zhou, et al., *IEEE Photonics Journal,* 2020, **12**, 5900408.
15. J. L. Qiu, X. Y. Liu, Z. Z. Liang, et al., *Optics Letters* 2021, **46**, 849-852.
16. L. Quan, C. H. Wang, Y. L. Xu, et al., *Chemical Engineering Journal,* 2022, **428**, 131337.
17. J. Q. Shen, F. J. Li, Z. B. Wang, et al., *Ieee Journal of Selected Topics in Quantum Electronics,* 2023, 29, 6900408.
18. J. Liu, W. Z. Ma, W. Chen, et al., *IEEE Access,* 2021, **9**, 92941-92951.
19. Z. B. Wang, W. Chen, X. Y. Liu, et al., *Talanta,* 2023, **264**, 124731.
20. Y. N. Xie, X. Y. Liu, J. Zhou, et al., Enhancing Trace Terahertz Fingerprint Sensing by the Lossy Silicon Metagrating With a Gold Mirror. *Ieee Transactions on Microwave Theory and Techniques* **2023**.

21. J. F. Zhu, S. Yan, N. X. Feng, et al., *Applied Physics Letters* 2018, **112**, 153106.
22. J. Liu, C. Dou, W. Chen, et al., *Solar Energy Materials and Solar Cells,* 2022, **244**, 111822.
23. X. Yao, S. Jiang, S. S. Luo, et al., *ACS Applied Materials & Interfaces,* 2020, **12**, 36505-36512.
24. J. Liu, W. Chen, W. Z. Ma, et al., *IEEE Access,* 2020, **8**, 43407-43412.
25. Q. Lu, X. Li, X. Zhang, et al., *Engineering*, 2022, **17**, 22-30.
26. L. Zhang, X. Q. Chen, S. Liu, et al., *Nature Communications*, 2018, **9**, 4334.
27. Y. Wang, W. Sha, M. Xiao, et al., *Advanced Materials*, 2023, 35(33): 2302387.
28. Y. Chen, Y. Ma, Q. Yin, et al., *Composites Science and Technology*, 2021, **214**, 108970.
29. J. F. Zhu, Z. Y. Wang, S. W. Lin, et al., *Biosensors & Bioelectronics,* 2020, **150**, 111905.
30. J. K. Xiong, J. Q. Shen, Y. Gao, et al., *Laser & Photonics Reviews,* 2023, **17**, 2100738.
31. W. Z. Ma, J. Liu, W. Chen, et al., *Results in Physics,* 2021, **31**, 105055.
32. J. F. Zhu, L. R. Zhang, S. Jiang, et al., *Nanoscale,* 2020, **12**, 2057-2062.
33. W. Chen, J. Liu, W. Z. Ma, et al., *Applied Sciences-Basel,* 2020, **10**, 3276.
34. Y. S. Chen, D. Meng, W. Z. Ma, et al., *Optics Express,* 2021, **29**, 37234-37244.
35. C. Dou, Z. C.Wu, W. Chen, et al., *Carbon,* 2024, **216**, 118556.
36. J. Liu, W. Chen, Y. S. Chen, et al., *Journal of Materials Research and Technology,* **2020,** *9* (3), 6723-6732.
37. O. A. M. Abdelraouf, A. P. Anthur, Z. Dong, et al., *Advanced Functional Materials,* 2021, **31**, 2104627.
38. Z. Dong, S. Gorelik, R. Paniagua-Dominguez, et al., *Nano Letters,* 2021, **21**, 4853-4860.
39. L. F. Ye, X. Chen, G. X. Cai, et al., *Nanomaterials,* 2018, **8**, 562.
40. M. Asbahi, Z. Mahfoud, S. B. Dolmanan, et al., *ACS Applied Materials & Interfaces,* 2019, 11, 45207-45213.
41. K. Yang, J. Y. Wang, X. Yao, et al., *Advanced Optical Materials,* 2021, **9**, 2001375.
42. J. Liu, C. Dou, W. Chen, et al., *Microchemical Journal,* 2022, **183**, 108043.
43. Z. B. Wang, J. J. Chen, S. A. Khan, et al., *Sensors,* 2022, **22**, 133.
44. J. Liu, W. Z. Ma, W. Chen, et al., *Optics Express,* 2020, **28**, 23748-23760.
45. Z. Dong, Z. Mahfoud, R. Paniagua-Dominguez, et al., Nanoscale mapping of optically

inaccessible bound-states-in-the-continuum. *Light-Science & Applications,* 2022, **11**, 20.
46. J. F. Zhu, L. R. Zhang, Y. Q. Bai, et al., *IEEE Photonics Technology Letters,* 2017, **29**, 504-506.
47. W. Z. Ma, J. Liu, G. X. Yu, et al., *Current Applied Physics,* 2021, **27**, 51-57.
48. D. Meng, J. Liu, W. Chen, et al., *Results in Physics,* 2022, **39**, 105766.
49. J. Liu, W. Chen, W. Z. Ma, et al., *Infrared Physics & Technology,* 2022, **127**, 104447.
50. Z. Dong, H. S. Chu, D. Zhu, et al., *ACS Photonics,* 2015, **2**, 385-391.
51. O. A. M. Abdelraouf, Z. Wang, H. Liu, et al., *ACS Nano,* 2022, 16, 13339–13369.
52. M. Asbahi, Z. Dong, F. Wang, et al., *Nanoscale,* 2017, 9, 9886-9892.
53. J. Liu, W. Chen, J. C. Zheng, et al., *Nanomaterials,* 2020, **10**, 27.
54. Z. Dong, M. Asbahi, J. Lin, et al., *Nano Letters,* 2015, **15**, 5976-5981.
55. Y. Liu, H. Wang, J. Ho, et al., *Nature Communications,* 2019, *10*, 4340.
56. M. Asbahi, F. Wang, Z. Dong, et al., *Nanotechnology,* 2016, 27, 424001.
57. Z. Dong, M. Bosman, D. Zhu, et al., *Nanotechnology,* 2014, **25**, 135303.
58. O. A. M. Abdelraouf, A. P. Anthur, H. Liu, et al., *2021 Conference on Lasers and Electro-Optics (CLEO)*, San Jose, CA, USA, 2021, 1-2
59. J. Liu, W. Chen, W. Z. Ma, et al., *Results in Physics,* 2021, **22**, 103818.
60. Z. Dong, J. Ho, Y. F. Yu, et al., *Nano Letters,* 2017, **17**, 7620-7628.
61. Z. Dong, L. Jin, S. D. Rezaei, et al., *Science Advances,* 2022, **8**, eabm4512.
62. W. Z. Ma, W. Chen, D. G. Li, et al., *Nanophotonics,* 2023, **12**, 3589-3601.
63. K. Huang, Z. Dong, S. Mei, et al., *Laser & Photonics Reviews,* 2016, **10**, 500-509.
64. Z. Dong, T. Wang, X. Chi, et al., *Nano Letters,* 2019, **19**, 8040-8048.
65. J. Gu, Y. Liu, N. Meng, et al., *Advanced Optical Materials,* 2023, **11**, 2202826.
66. R. He, M. Meunier, Z. Dong, et al., *Nanoscale,* 2023, **15**, 1652-1660.
67. J. Ho, Y. H. Fu, Z. Dong, et al., *ACS Nano,* 2018, **12**, 8616-8624.
68. Z. Ding, W. Su, F. Hakimi, *Solar Energy Materials and Solar Cells*, 2020, **262**, 112563.
69. K. Huang, D. Zhao, F. Tjiptoharsono, et al., *ACS Nano,* 2020, **14**, 7529-7537.
70. M. Jalali, Y. Yu, K. Xu, et al., *Nanoscale,* 2016, **8**, 18228-18234.
71. N. Yu, P. Genevet, M. A. Kats, et al., Science, 2011, 334(6054), 333-337.
72. L. Jiang, T. Yin, Z. Dong, et al., *ACS Nano,* 2015, **9**, 10039-10046.

73. L. Jin, Z. Dong, S. Mei, et al., *Nano Letters,* 2018, **18**, 8016-8024.
74. L. Jiang, T. Yin, A. M. Dubrovkin, et al., In-plane coherent control of plasmon resonances for plasmonic switching and encoding. *Light-Science & Applications* 2019, **8**, 21.
75. L. Jin, Y. W. Huang, Z. Jin, et al., *Nature Communications,* 2019, **10**, 4789.
76. C. Jung, G. Kim, M. Jeong, et al., *Chemical Reviews,* 2021, **121** (21), 13013-13050.
77. S. Kruk, L. Wang, B. Sain, et al., *2021 Conference on Lasers and Electro-Optics (CLEO)*, San Jose, CA, USA, 2021, 1-2.
78. S. S. Kruk, L. Wang, B. Sain, et al., *Nature Photonics,* 2022, **16**, 561.
79. H. Liu, H. Wang, H. Wang, et al., *Acs Nano,* 2022, **16** (5), 8244-8252.
80. M. Limonov, M. Rybin, A. Poddubny, et al. *Nature Photonics*, 2017, **11**, 543-554.
81. Z. Ding, W. Su, L. Ye, *Solar Energy*, 2024, **271**, 112449.
82. B. Wang, R. An, E. A. Chan, et al., arXiv preprint arXiv: 2023, 2311, 10441.
83. L. Lu, Z. Dong, F. Tijiptoharsono, et al., *Acs Nano,* 2021, **15**, 19722-19732.
84. H. K. Ng, D. Xiang, A. Suwardi, et al., *Nature Electronics,* 2022, **5**, 489-496.
85. R. J. H. Ng, R. V. Krishnan, Z. Dong, et al., *Optical Materials Express,* 2019, **9**, 788-801.
86. S. D. Rezaei, Z. Dong, J. Y. E. Chan, et al., *ACS Photonics,* 2021, **8**, 18-33.
87. Z. Wang, Z. Dong, Y. Gu, et al., *Nature Communications,* 2016, **7**, 11283.
88. S. D. Rezaei, J. Ho, A. Naderi, et al., *Advanced Optical Materials,* 2019, **7**, 1900735.
89. X. Yu, Z. Dong, J. K. W.Yang, et al., *Optica,* 2016, **3**, 979-984.
90. X. Su, Z. Dong, J. Wu, et al., *ACS Nano,* 2022, **16**, 11492-11497.
91. J. Tao, Z. Dong, J. K. W. Yang, et al., *Optics Express,* 2015, **23**, 7809-7819.
92. J. Trisno, L. Lu, Z. Dong, et al., *ACS Photonics,* 2018, **5**, 511-519.
93. T. Wang, Z. Dong, E. H. H. Koay, et al., *ACS Photonics* 2019, **6**, 1272-1278.
94. S. D. Rezaei, Z. Dong, H. Wang, et al., *Materials Today,* 2023, **62**, 51-61.
95. Z. Wang, Z. Dong, H. Zhu, et al., *Acs Nano,* 2018, **12**, 1859–1867.
96. X. Xiong, Y. Lai, D. Clarke, et al., *Advanced Optical Materials,* 2022, **10**, 2200557.
97. J. Xu, Z. Dong, M. Asbahi, et al., *Nano Letters,* 2021, **21**, 3044-3051.
98. P. Y. M. Yew, D. D. Zhu, Q. Y. Lin, et al., *Materials Today Chemistry,* 2021**, 22**, 100574.
99. T. Yin, Z. Dong, L. Jiang, et al., *ACS Photonics,* 2016, **3**, 979-984.
100. T. Yin, L. Jiang, Z. Dong, et al., *Nanoscale,* 2017, **9**, 2082-2087.

101. X. Yu, Z. Dong, Y. Liu, et al., *Nanoscale,* 2016, **8**, 327-332.

102. S. D. Rezaei, R. J. H. Ng, Z. Dong, et al., *ACS Nano,* 2019, **13**, 3580-3588.

103. X. Yu, Z. Dong, J. K. W. Yang, et al., *2016 Conference on Lasers and Electro-Optics (CLEO)*, San Jose, CA, USA, 2016, 1-2.

104. L. Zhang, Z. Dong, Y. M. Wang, et al., *Nanoscale,* 2015, **7**, 12018-12022.

105. S. Zhang, J. Zhang, W. P. Goh, et al., *Nanophotonics,* 2023, **12**, 1387-1395.

106. D. Zhao, Z. Dong, K. Huang, *Optics Letters,* 2021, **46**, 1462-1465.

107. D. Zhu, Z. Dong, H. S. Chu, et al., *ACS Photonics,* 2014, **1**, 1307-1312.

108. Q. Zhu, M. H. Chua, P. J. Ong, et al., *Materials Today Advances,* **2022,** *15*, 100270.

109. S. Molesky, Z. Lin, A.Y. Piggott, et al., *Nature Photonics* 2018, **12**, 659-670.

110. W. Ma, Z. Liu, Z. A. Kudyshev, *Nature Photonics*, 2021, **15**, 77-90.

111. D. Lee, S. So, G. Hu, et al., *ELight*, 2022, **2**, 1-23.

112. E. Galiffi, G. Carini, X. Ni, et al. *Nature Reviews Materials*, 2024, **9**, 9-28.

113. X. R. Mao, Z. K. Shao, H. Y. Luan, et al., *Nature Nanotechnology*, 2021, **16**, 1099-1105.

114. L. Huang, R. Jin, C. Zhou, et al., *Nature Communications*, 2023, **14**, 3433.

115. T. Kaelberer, V. A. Fedotov, N. Papasimakis, et al., *Science*, 2010, **330**, 1510-1512.

116. A. R. Indhu, L. Keerthana, G. Dharmalingam, *Beilstein Journal of Nanotechnology*, 2023, **14**, 380-419.

117. Y. Ke, B. Zhang, T. Wang, et al., *Materials Horizons*, 2021, **8**, 1700-1710.

118. K. Zhang, Y. Liu, F. Xia, et al., *Optics Letters*, 2020, 45, 3669-3672.

119. T. T. Hoang, Q. M. Ngo, D. L.Vu, et al., *Scientific Reports*, 2018, **8**, 16404.

120. B. Luk'Yanchuk, N. I. Zheludev, S. A. Maier, et al., *Nature materials*, 2010, **9**, 707-715.

121. G. Hu, X. Hong, K. Wang, et al., *Nature Photonics*, 2019, **13**, 467-472.

122. K. V. Sreekanth, Y. Alapan, M. ElKabbash, et al., *Nature Materials*, 2016, **15**, 621-627.

123. G. Hu, Q. Ou, G. Si, et al., *Nature*, 2020, **582**, 209-213.

124. G. Hu, A. Krasnok, Y. Mazor, et al., *Nano Letters*, 2020, **20**, 3217-3224.

125. Q. Zhang, G. Hu, W. Ma, et al., *Nature*, 2021, **597**, 187-195.

126. G. Hu, W. Ma, D. Hu, et al. *Nature Nanotechnology*, 2023, **18**, 64-70.

127. A. E. Miroshnichenko, A. B. Evlyukhin, Y. F. Yu, et al., *Nature Communications*, 2015, **6**, 8069.

128. T. Zhan, X. Shi, Y. Dai, et al., *Journal of Physics: Condensed Matter*, 2013, **25**, 215301.

129. M. Nieto-Vesperinas, Dielectric Metamaterials. Woodhead Publishing, 2020: 39-72.

130. K. S. Kunz, R. J. Luebbers, CRC Press, 1993.

131. F. L. Teixeira, C. Sarris, Y. Zhang, et al., *Nature Reviews Methods Primers*, 2023, **3**, 75.

132. M. N. Ab Wahab, S. Nefti-Meziani, A. Atyabi, *PloS one*, 2015, **10**, e0122827.

133. L. Huang, L. Xu, A. E. Miroshnichenko, *Advances and Applications in Deep Learning*, 2020, **65**, 1-14.

134. J. Peurifoy, Y. Shen, L. Jing, et al., *Science Advances,* 2018, **4**, eaar4206.

135. C. Qian, B. Zheng, Y. Shen, et al., *Nature. Photonics*, 2020, **14**, 383-390.

136. Ma, W.; Xu, Y.; Xiong, B. et al., *Advanced Materials*, 2022, **34**, 2110022.

137. H. H. Yoon, H. A. Fernandez, F. Nigmatulin, et al., *Science*, 2022, **378**, 296-299.

138. J. Hu, S. Bandyopadhyay, Y. Liu, et al., *Frontiers in Physics*, 2021, **8**, 586087.

139. E. Csányi, Y. Liu, S. D. Rezaei, et al., *Advanced Functional Materials*, 2024, **34**, 2309539.

140. J. Ho, Z. Dong, H. S. Leong, et al., *Science Advances*, 2022, **8**, eadd3868.

141. T. Santiago-Cruz, S. D. Gennaro, O. Mitrofanov, et al., *Science*, 2022, **377**, 991-995.

142. A. Leitis, M. L. Tseng, A. John-Herpin, et al., *Advanced Materials*, 2021, **33**, 2102232.

143. J. Mandal, Y. Fu, A. C. Overvig, et al., *Science*, 2018, **362**, 315-319.

144. K. Koshelev, S. Kruk, E., *Science*, 2020, **367**, 288-292.

145. C. Huang, C. Zhang, S. Xiao, et al., *Science*, 2020, **367**,1018-1021.

146. P. Corbae, S. Ciocys, D. Varjas, et al., *Nature Materials*, 2023, **22**, 200-206.

147. X. Zhang, Y. Liu, J. Han, et al., *Science*, 2022, **377**, 1215-1218.

148. A. Kodigala, T. Lepetit, Q. Gu, et al., *Nature*, 2017, **541**, 196-199.

149. Z. Gan, H. Feng, L. Chen, et al., *Light: Science & Applications*, 2022, **11**, 89.

150. M. Song, L. Feng, P. Huo, et al., *Nature Nanotechnology*, 2023, **18**, 71-78.

151. K. Kumar, H. Duan, R. S. Hegde, et al., *Nature Nanotechnology*, 2012, **7**, 557-561.

152. L. Lu, Z. Dong, F. Tijiptoharsono, et al., *ACS Nano*, 2021, **15**, 19722-19732.

153. Y. Liu, H. Wang, J. Ho, et al., *Nature Communications*, 2019, **10**, 4340.

154. A. Kristensen, J. Yang, S. Bozhevolnyi, et al., *Nature Reviews Materials*, 2017, **2**, 16088.

155. S. Zhang, J. Zhang, W. P. Goh, et al., *Nanophotonics*, 2023, **12**, 1387-1395.

156. S. D. Rezaei, Z. Dong, H. Wang, et al., *Materials Today*, 2023, **62**, 51-61.

157. A. Azzouz, L. Hejji, K. H. Kim, et al., *Biosensors and Bioelectronics*, 2022, **197**, 113767.

158. S. Ferguson, K. S. Yang, P. Zelga, et al., *Science Advances*, 2022, **8**, eabm3453.

159. Y. Fan, X. Duan, M. Zhao, et al., *Biosensors and Bioelectronics*, 2020, **154**, 112066.

160. M. H. Jeong, T. Son, Y. K. Tae, et al., *Advanced Science*, 2023, **10**, 2205148.

161. C. Jiang, Y. Fu, G. Liu, et al., *Nano-Micro Letters*, 2021, **14**, 3.

162. C. Z. J. Lim, Y. Zhang, Y. Chen, et al., *Nature Communications*, 2019, **10**, 1144.

163. Y. Ren, K. Ge, D. Sun, et al., *Biosensors and Bioelectronics*, 2022, **199**, 113870.

164. A. Natalia, L. Zhang, N. R. Sundah, et al., *Nature Reviews Bioengineering*, 2023, **1**, 481.

165. A. Thakur, C. Xu, W. K. Li, et al., *Biosensors and Bioelectronics*, 2021, **191**, 113476.

166. J. Wang, A. Wuethrich, A. A. I. Sina, et al., *Science Advances*, 2020, **6**, eaax3223.

167. Q. Wang, L. Zou, X. Yang, et al., *Biosensors and Bioelectronics*, 2019, **135**, 129-136.

168. J. Hu, F. Safir, K. Chang, et al., *Nature Communications*, 2023, **14**, 4486.

169. Y. Jahani, E. R. Arvelo, F. Yesilkoy, et al., *Nature Communications*, 2021, **12**, 3246.

170. S. Pan, Y. Zhang, A. Natalia, et al., *Nature Nanotechnology,* 2021, **16**, 734-742.

171. F. Li, J. Hong, C. Guan, et al., *ACS Nano*, 2023, **4**, 3383.

172. X. Liu, Y. Xie, J. Qiu, et al., *Nanophotonics,* 2023, **12**, 4319-4328.

173. Z. Liu, T. Guo, Q. Tan, et al., *Nano Letters*, 2023, **23**, 10441-10448.

174. L. Sun, L. Xu, J. Wang, et al., *Nanoscale*, 2022, **14**, 9681-9685.

175. M. Zheng, Y. Shen, Q. Zou, et al., *Advanced Functional Materials*, 2022, **33**, 2209368.

176. A. Tittl, A. Leitis, M. Liu, et al., *Science* 2018, **360**, 1105.

177. A. Aigner, A. Tittl, J. Wang, et al., *Science Advances*, 2022, **8**, eadd4816.

178. J. Lyu, S. Shen, L. Chen, et al., *PhotoniX*, 2023, **4**, 28.

179. Y. Ke, X. Wen, D. Zhao, et al., *ACS Nano*, 2017, **11**, 7542-7551.

180. Y. Ke, Y. Yin, Q. Zhang, et al., *Joule*, 2019, **3**, 858-871.

181. Y. Ke, T. Wang, N. Li, et al., *Optics Express*, 2021, **29**, 9324-9331.

182. Z. Dong, T. Wang, X. Chi, et al., *Nano Letters*, 2019, **19**, 8040-8048.

183. X. Ding, Z. Zhao, P. Xie, et al., A*dvanced Materials*, 2024, **36**, 2308993.

184. X.Wang, H.Wang, J. Wang, et al. *Nature communications*, 2023, **14**, 2063.

185. Z.Wang, G. Hu, X. Wang, et al. *Nature communications*, 2022,**13**, 2188.